

Wear analysis of NbC-Ni cemented carbides for cutting tools

Laerte Jose Fernandes , Rodrigo Lima Stoeterau , Gilmar Ferreira Batalha , Daniel Rodrigues & Anderson Vicente Borrile

To cite this article: Laerte Jose Fernandes , Rodrigo Lima Stoeterau , Gilmar Ferreira Batalha , Daniel Rodrigues & Anderson Vicente Borrile (2020): Wear analysis of NbC-Ni cemented carbides for cutting tools, Advances in Materials and Processing Technologies, DOI: [10.1080/2374068X.2020.1808925](https://doi.org/10.1080/2374068X.2020.1808925)

To link to this article: <https://doi.org/10.1080/2374068X.2020.1808925>



Published online: 01 Sep 2020.



Submit your article to this journal [↗](#)



View related articles [↗](#)



View Crossmark data [↗](#)



Wear analysis of NbC-Ni cemented carbides for cutting tools

Laerte Jose Fernandes^a, Rodrigo Lima Stoeterau^a, Gilmar Ferreira Batalha^a, Daniel Rodrigues^b and Anderson Vicente Borrile^c

^aSchool of Engineering, University of Sao Paulo, São Paulo, Brazil; ^bBRATS Co., Cajamar, Brazil; ^cBrazil Praça Marechal Eduardo Gomes, CCM-ITA São José Dos Campos, SP, São José Dos Campos, Brazil

ABSTRACT

This research had the objective of investigating the viability of using Niobium Carbide – Nickel binder cemented carbides as an alternative material for cutting tools. The high hardness and high wear resistance associated with Niobium carbide – NbC, fulfil one of the main requirements for cutting tool material. In order to achieve this objective, insert tools with square shapes were manufactured using samples at five different grades. The samples were developed with different ratios of NbC carbide/Ni binder, compaction parameters and sintering conditions. The samples were qualified in terms of microhardness and physical properties. The inserts were also qualified in terms of their macro-geometry, surface finish, cutting edge micro-geometry. Machining experiments were performed under different cutting parameters on tempered ANSI 4340 steel workpieces. Flank wear progression was the control parameter, and the wear analyses were made using a CCD camera and SEM/EDS. The main wear mechanisms observed were abrasion, followed by adhesion, while no traces of tribo-oxidation and diffusion were observed. The results led to the conclusion that the NbC carbide/Ni binder ratio had the greatest influence on wear, but the leading parameter was the sintering conditions.

ARTICLE HISTORY

Accepted 9 August 2020

KEYWORDS

Niobium carbide; nickel; cemented carbides; wear; powder metallurgy; machining

1. Introduction

In order to meet the increasing demand for products for various industrial applications, there are several different processes, such as casting, forming, machining and welding. In the machining process, the precision of the mechanical parts is extremely important since all parts have to attain the required levels of accuracy [1,2].

During the tool cutting process, there is an increase in temperature at the cutting tool/workpiece interface due to low thermal conductivity, highest at the cutting edge but not completely dissipating into chips and workpieces. As a result, there is great cutting edge wear which reduces the useful life of the cutting tool. The cutting tool material and its geometry are significant in the machining process with regard to machinability [3]. Other important factors are the material of the cutting tool, the machining parameters, and whether the wetting condition is dry or uses coolant [3].

CONTACT Laerte Jose Fernandes  laertejf@usp.br; fernandes.laerte@yahoo.com.br  School of Engineering, University of Sao Paulo, São Paulo, SP 2232, Brazil

© 2020 Informa UK Limited, trading as Taylor & Francis Group

Cutting tools are subjected to enormous strain, high temperatures, high contact pressure and different wear conditions during the chip formation. The main requirements desirable for cutting tool materials are: hardness and pressure resistance, bending strength and toughness, edge strength and inner bonding strength. For cemented carbide tools, the following are important: high-temperature strength, oxidation resistance, small propensity to diffusion and adhesion, abrasion resistance and reproducible wear behaviour.

No existing tool material is able to fulfil all these requirements simultaneously. The development of a new cutting material must attain a compromise solution between hardness and toughness [4,5].

Cemented carbide tools first appeared in 1927, and were developed by Widia Co. They were primarily used for machining cast iron, due to their high crater wear resistance [4]. Later, their use was extended to machining long chip formation materials, such as steel and aluminium alloys.

Niobium carbide has been used as a secondary hard phase material in high-speed steels, cemented tungsten carbides and titanium cermet tools, but its potential as a main hard phase in cutting tools has barely been explored. The hardness of Niobium carbide is comparable to that of Titanium, Tungsten, Molybdenum and Chromium carbide. Its high hardness provides high wear resistance desirable for cutting tool applications. On the other hand, its low solubility and high sintering temperatures are two key points which have to be overcome. The improvement in sintering techniques has enabled the exploration of its full potential as a cutting tool material. A hot-pressing process, high-frequency induction heated sintering and spark-plasma-sintering (SPS) allow high-quality NbC based carbides to be obtained.

This work had the objective of comparing the cutting performance of five alternative NbC-Ni-based cemented inserts with different combinations of carbides, and sintering conditions, in relation to an equivalent tungsten carbide tool. To achieve this objective, five types NbC-Ni-based cemented inserts were developed, and machining tests were performed using high alloy steel AISI 4340 quenched and tempered, hardness of 320 ± 20 HB, as the test material. The progression of the flank wear was used as a comparison parameter, to determine the wear resistance performance.

2. Cemented carbide tool

2.1. Cemented carbide tools and their properties

Cemented carbide is a family of composite materials, manufactured by powder-metalurgy in which the main hard phase is provided by a carbide, which provides the hardness, cemented by a binder, which gives the material toughness and plasticity [6].

To improve some specific requirements, such as increasing the toughness of the carbide (γ phase), or the high-temperature strength, second phase carbides as TiC, TaC, MoC, NbC are added. Cobalt is the main binder phase for cemented carbides based on tungsten carbide. This is due to the high level of solubility of WC in cobalt and to the good wettability of tungsten carbide crystals by the molten WC-Co binder. Nickel can also be used as a binder due to the improved wettability of hard materials, such as carbides. Comparing the two, Nickel is more deformable than Cobalt, and nowadays

cobalt is added with nickel as a binder in cement in order to improve the high-temperature strength. It can also be replaced by iron [4,6,7].

2.2. WC hard phase microstructural components in cemented carbides

W-C and W-Co-C systems belong to the group of non-stoichiometric interstitial compounds [8]. Mono tungsten carbide is the most important hard phase of the cemented carbide. The WC solubility in Co results in the high internal bond strength and the resistance of the cemented carbide WC-Co cutting edges. Comparatively, the wear resistance of WC is higher than TiC and TaC.

In terms of machining, the cutting speed is limited at higher temperatures due to the tendency of WC to have problems associated with chemical affinity and diffusion [4].

The properties of WC and especially its thermal stability during heating up to 1,000–1,200 K determine the use of WC for producing wear-resistant cemented carbides, which are, in fact, most tool materials. The direct use of WC carbide as a cutting tool material is impossible due to its brittleness and sintering at very high temperatures [8]. The properties of tungsten carbide in the cemented carbide (WC-Co) depend mainly on the microstructure, especially its cobalt content and WC grain size [9].

2.3. NbC cemented carbide tools

Niobium carbide (NbC) is used as the secondary phase of carbide, to increase wear resistance, improving hot hardness and limiting grain growth. However, recent pieces of research have shown that niobium carbide has important tribological, physical and mechanical properties for cutting tool applications that could be used instead of tungsten carbide, which has long been used in this application [10–12].

Recently, special attention has been given to the use of niobium for cutting tool applications, using niobium carbide (NbC) as the main hard phase of the cutting tool substrate. Some of the properties of niobium carbide were compared with those of tungsten carbide. Niobium carbide has some distinct advantages over this established cutting material. However, the mechanical and particularly tribological properties of NbC remain largely unexplored. In a preliminary analysis, the applications in NbC cutting tools should be superior to WC, because at 1,225°C, NbC is almost insoluble in Cr, Ni, Co or Fe, while WC is totally soluble under the same conditions. The high solubility of WC in these metals is responsible for the chemical wear (diffusion) of the WC. Its higher melting point and the tribo-oxidative formation of niobium oxide (Nb₂O₅) on the tool surface, in combination with low solubility of NbC in metals, lead to a reduced tendency to adhesive and diffusion wear [10,11].

Little attention has been given to niobium carbide research, although some research was conducted in the 1960s and 1970s. This suggests that availability and prices at that time were prohibitive. However, the global situation with regard to niobium carbide has changed significantly because niobium is now an indispensable element of microalloying for steel pipes, steel for car bodies of high-strength steels for structural applications, with a total sales volume of 85,000 tons per year, and this has led to further research [10,13].

Currently, Niobium also has a very important benefit in relation to sustainability (the environment). Niobium oxide (Nb₂O₅) and niobium carbide (NbC) present no risks or

critical notifications on REACH – Registration, Evaluation, Authorisation and Restriction of Chemical Substances Programme. REACH is a European Union regulation aiming to improve the protection of human health and the environment from the risks posed by chemicals. Niobium carbide has not been restricted by any critical rating to date. Conversely, compositions used to obtain WC-Co powder by reduction processes, such as tungsten trioxide (WO_3) and tricobalt tetroxide (Co_3O_4), received various adverse classifications and were referred to in various reports because of their relationship with mutagenic, carcinogenic toxicity and reproductive toxicity rates by REACH [10–12,14].

2.4. Niobium cemented carbides microstructural components

NbC can form cubic sub-carbides, making a wide range of carbon stoichiometry possible, as can be seen in Figure 1, which shows the binary phase diagram Nb-C. It can thus be adapted by stoichiometry in the range of NbC to $\text{NbC}_{0.75}$ properties, such as hardness, elasticity modulus and others. The possibility of working in this range, adjusting the C/Nb ratio, may also contribute to NbC powder manufacturing, as a wider range of carbon content can be used.

According to Woydt et al. [10] with decreasing C/Nb ratio, hardness markedly increases but the modulus of elasticity decreases. Figure 2 shows the sub-stoichiometric influence of NbC on microhardness. Unlike the binary phase diagram C/Nb, the binary phase diagram W-C presents a restricted range of carbon content to form the tungsten carbide used in the cutting tool material. There is, therefore, a greater difficulty for the manufacture of WC powders, because the carbon must be correctly added in order to avoid there being too little carbon to form tungsten carbide.

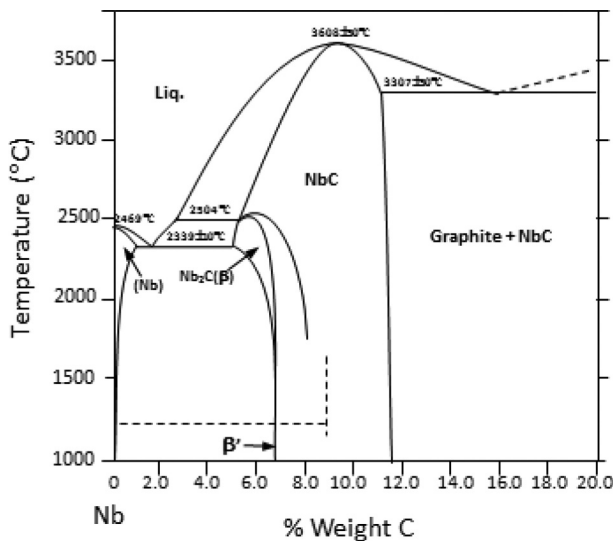


Figure 1. Binary Nb-C phase diagram [15].

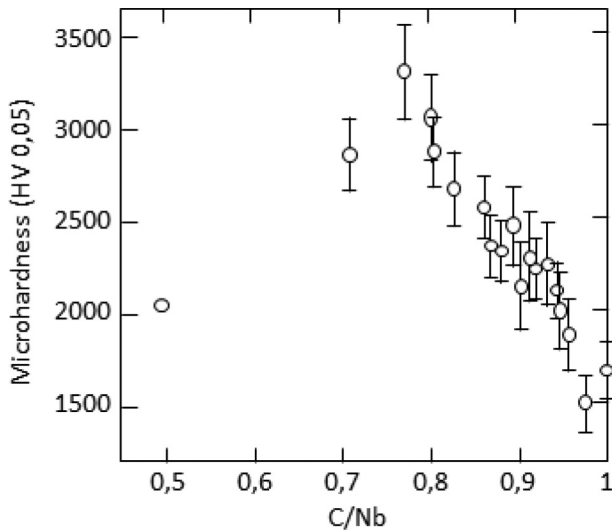


Figure 2. Micro-hardness of NbC phases as a function of C/Nb ratio [16].

3. Materials and methods

3.1. Development of NbC-Ni cemented carbide tools

Insert tools with five different cemented NbC carbide grades, binders and sintering conditions were developed. Table 1 presents the composition, hardness, fracture toughness, sintering furnace atmosphere, threshold time, sintering temperature, density and relative density. The sintering process in the liquid phase was used for the manufacture of cutting tools based on NbC-Ni through sintering cycles were done under vacuum and under dynamic inert gas.

These cycles are shown in Figure 3(a, b). The sintering cycle was performed under vacuum conditions (Figure 3(a)), where a high evaporation of nickel was observed. This could lead to unexpected variations in the mechanical properties. In order to reduce nickel losses during sintering, an Argon dynamic atmosphere was introduced for the

Table 1. Composition, hardness, fracture toughness, sintering furnace atmosphere, threshold time, sintering temperature, density and relative density for the NbC-Ni developed tools.

ID	Composition (%w)	Hardness HV ₃₀	K _{IC} (MPa·m ^{1/2})	Atm	T _{sinter} (min)	t _{sinter} (°C)	Density (g/cm ³)	Relative density (%)
900	15%Ni +12%WC +14%TiC +59% NbC	1289 ± 23	10.2 ± 0.7	V	15	1420	7.58	97.6
938	15%Ni +12%WC +14%TiC +59% NbC	1440 ± 40	11.1 ± 0.3	V	20	1420	7.71	99.1
959	12%Ni +12%WC +14%TiC + 62% NbC 7.59	1443 ± 32 97.9	9.0 ± 0.3	V	+ Ar	20	V -	1380 Ar - 1420
965	12%Ni +12%WC +14%TiC + 62% NbC 7.48	1280 ± 30 97.2	8.7 ± 0.4	V	+ Ar	15	V -	1380 Ar - 1420
967	10%Ni +12%WC +14%TiC + 64% NbC 7.60	1460 ± 40 97.9	8.9 ± 0.4	V	+ Ar	20	V -	1380 Ar - 1420

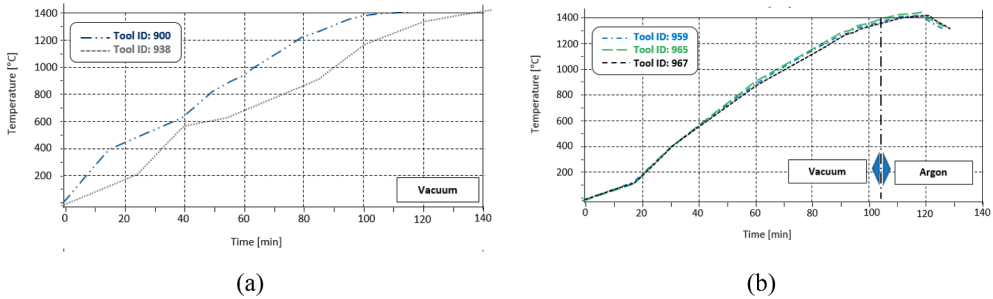


Figure 3. (a) Sintering process under vacuum; (b) Sintering process with dynamic inert gas.

Table 2. Per cent average by weight of chemical elements after sintering – EDS.

Sintering process	Grades	Ti (%w)	Ni (%w)	Nb (%w)	W (%w)	Ni-depletion (%)
Vacuum	NbC-Ni_900 (Ni –15%w)	13.4	13.8	57.8	11.8	8.0
Vacuum	NbC-Ni_938 (Ni –15%w)	13.5	13.7	57.6	11.7	8.7
Vacuum + Argon	NbC-Ni_959 (Ni –12%w)	13.3	11.6	61.4	11.8	3.3
Vacuum + Argon	NbC-Ni_965 (Ni –12%w)	13.7	11.5	61.2	11.6	4.2
Vacuum + Argon	NbC-Ni_967 (Ni –10%w)	13.6	9.8	63.8	11.6	2.0

sintering cycle (Figure 3(b)). The use of Argon minimises nickel depletion and promotes a better control of the nickel content after sintering. Table 2 presents the analysis of the weight percentage of the sample classes of the cutting tools based on NbC-Ni, performed via EDS in the SEM. The results were average values, and it can be observed that there was a greater evaporation of Ni in the vacuum sintering than under dynamic inert gas. The relative density of most of the NbC-Ni classes was in the range of 97.2% to 97.8%, only the NbC-Ni_938 class was above 99%. For each sintering process, heating temperature and sintering dwell time were also variable.

This allowed variations in the mechanical properties of the cutting materials to be obtained. Depending on the sintering dwell time, the hardness can decrease mainly as a result of grain growth, or it can allow an increase in dissolution of niobium into the nickel binder, increasing its hardness and decreasing the toughness. A compromise solution was obtained between these two phenomena.

A commercial grade WC-Co insert was used as a control tool, to set a reference for performance and reproducibility of results. Its measured hardness was $1670 \pm 5 \text{ HV}_{30}$, and fracture toughness K_{IC} : $10.3 \pm 0.1 \text{ MPa}\cdot\text{m}^{1/2}$.

Figure 4 shows as micrographs of the classes of NbC-Ni and WC-Co, reference in the optical microscope. It is possible to verify that there are small formations of nickel lakes (binder) in the NbC-Ni classes, which were not detected in the WC-Co class sample.

Figure 5 presents a more detailed comparison of the class NbC-Ni and WC-Co. In Figure 5(a), NbC-Ni_967, the nickel that is the binder, involved the carbides according to the details presented inside the circles (L1_Ni; L2_Ni; L3_Ni; L4_Ni). The wetting behaviour of nickel to bond carbide surfaces is of great importance because it allows us to understand how the metal will diffuse and dissolve during the liquid phase. This makes it possible to obtain high-density sinter. In Figure 6(a), an NbC matrix with well-defined grain boundaries can be observed and it is possible to verify in more detail the effect of nickel wettability in carbides,

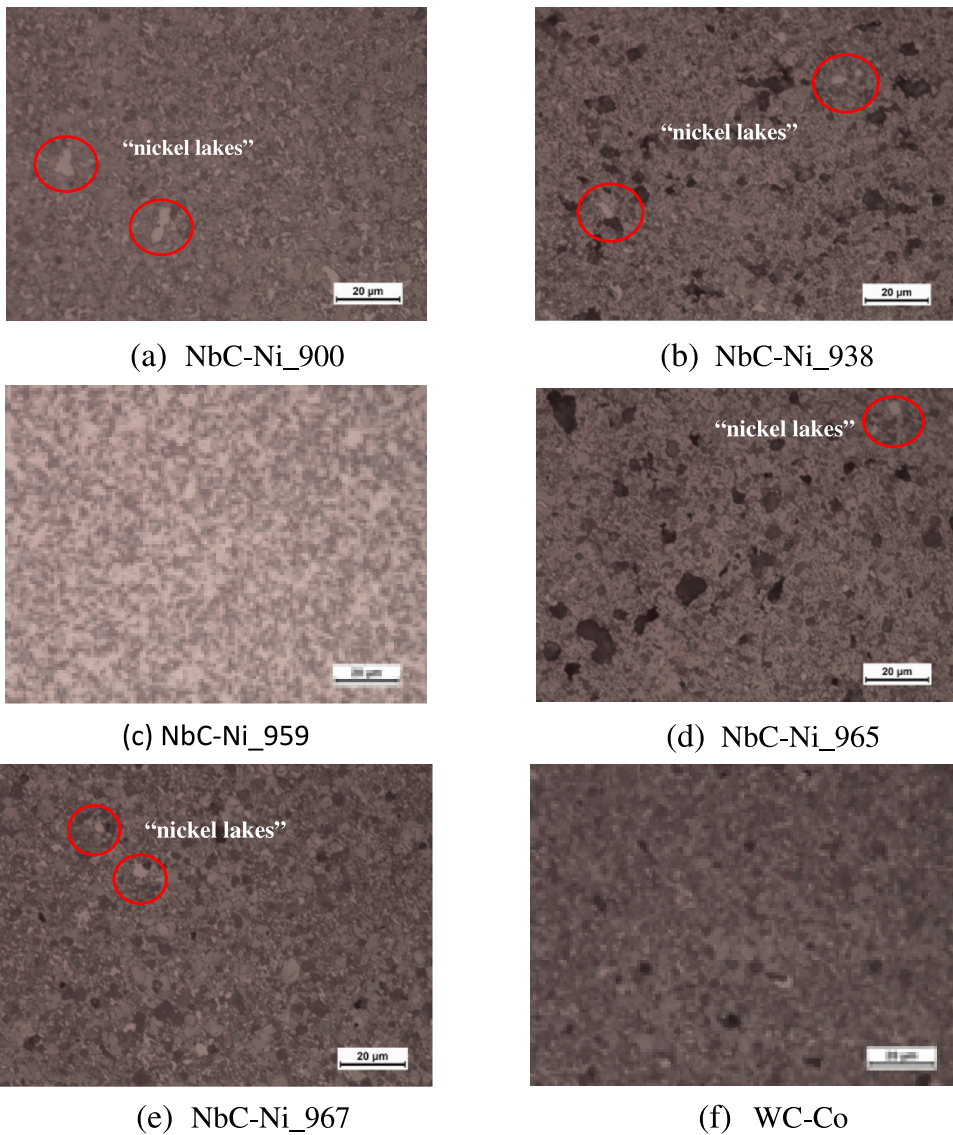


Figure 4. Micrograph of the NbC-Ni classes and WC-Co reference – Optical Microscope.

as in the grain boundaries typical micro-porosities of the structure obtained by solidification can be observed. In [Figures 5\(b\)](#) and [6\(b\)](#), WC-C it is possible to verify the same phenomenon in relation to cobalt, a binder of the WC, with the same behaviour of wettability.

The distribution of the second phase carbides became heterogeneous in the NbC-Ni Class, as can be seen in [Figure 6\(c\)](#), highlighted within the squares, in these cases at a concentration of tungsten carbides in certain regions. This is usually due to time and the effect of liquid (isopropyl alcohol) on the dispersion of particles in the milling process (attritor mill). In [Figures 4\(f\)](#) and [5\(b\)](#), WC-Co, the structure is homogeneous for carbides.

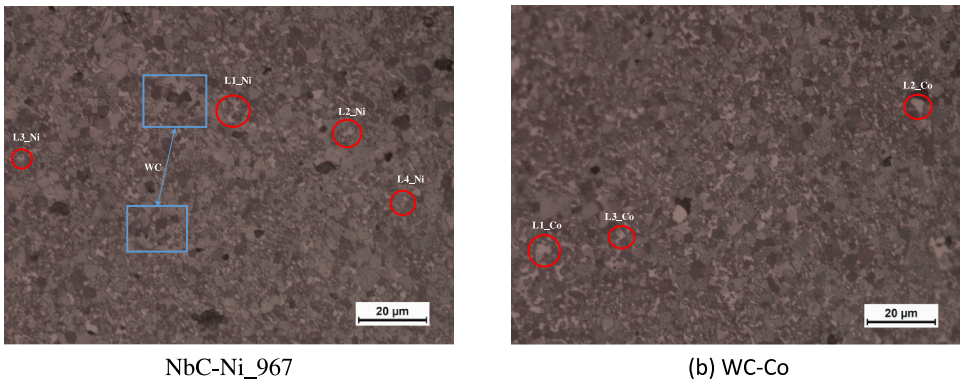


Figure 5. Comparison between the NbC-Ni class (NbC-Ni_967) and WC-Co reference.

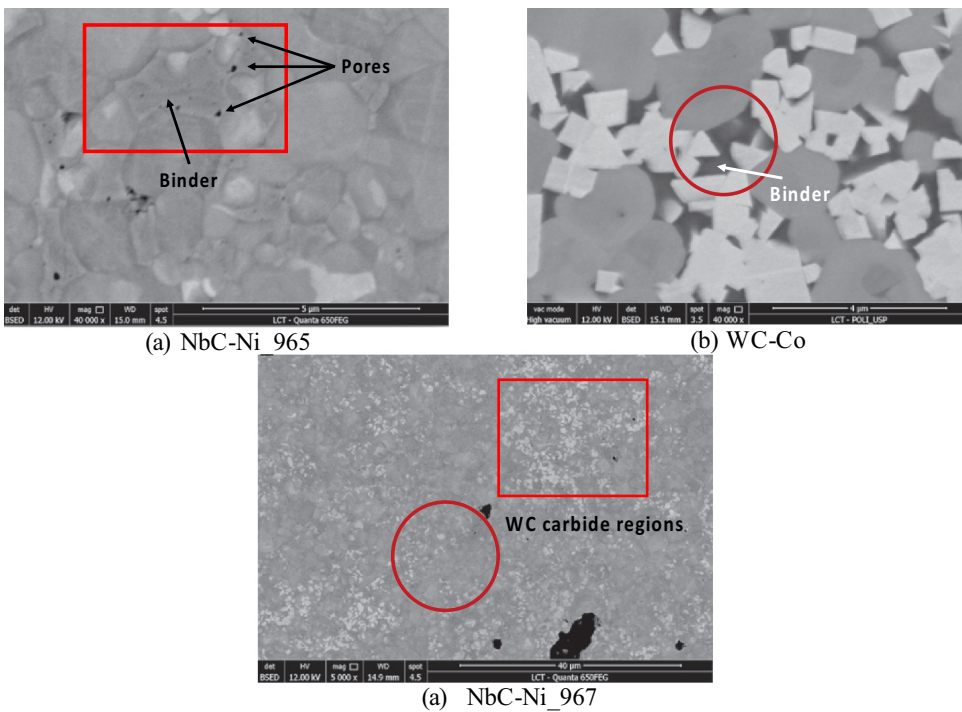
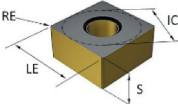
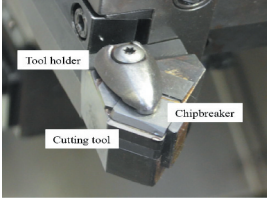


Figure 6. Detail of the microstructures.

The flank wear evolution was selected as a control parameter to evaluate the performance of the cutting tools developed. A square shape was selected as the primary form for the developed inserts, according to DIN ISO 1832 [4]. The geometries were SNMA190,608 and SNMN 190608. Fine grinding was done after sintering in order to attain the specified tolerances of shape and dimensions. The tool geometry, considering a tool-in-use system, is shown in Table 3.

Table 3. Insert dimensions and tool geometry considering a tool-in-use system.

Dimensions (mm)			
LE	19		
IC	19		
S	6		
RE	0.8		
		Relief angle Working cutting edge angle Rake angle Clearance angle Cutting direction Chip break	0° 45° -8° 0° Left External

3.2. Machining experiments

Flank wear evolution was carried out using turning experiments. Flank wear was measured on a pre-defined set of time. The test material had a 90 mm diameter, 325 mm length ANSI 4340 steel bar, tempered and quenched with a hardness of 320 ± 20 HB. Table 4 shows the microstructure of AISI 4340, etched with a 3% Nital solution (3% HNO₃ + 97% alcohol), and its composition. The results were compared to a WC-Co control tool. The flank wear progression was measured directly at the machine, with a CCD camera assembled on the tool holder. A 1,024 x 728 pixels resolution CCD camera, with a magnification of 200x, was used. The images were processed using dedicated software. Figure 7 shows the workflow of the experiments.

Preliminary experiments were conducted to establish the optimum cutting parameters range for the wear test. The preliminary parameters were $vc_1 = 160$ m/min, $vc_2 = 200$ m/min, $vc_3 = 250$ m/min, with a feed rate $f = 0.10$ mm/rev, and constant cutting depth $ap = 1.5$ mm, with lubrication. Water-miscible vegetable oil, ester-oil-based, free of chlorine, boron, formaldehyde and zinc, with a concentration of 10% and pH 9, was

Table 4. Microstructure and composition of AISI 4340 steel used in the experiments.

	C	Mn	Si	P	S	Cr	Ni	Mo	Fe
Workpiece	0.39	0.6	0.23	0.013	0.003	0.73	1.9	0.25	Bal
Standard	0.38–0.43	0.60–0.8	0.15–0.35	≤0.035	≤0.04	0.7–0.9	1.65–2.0	0.2–0.3	Bal

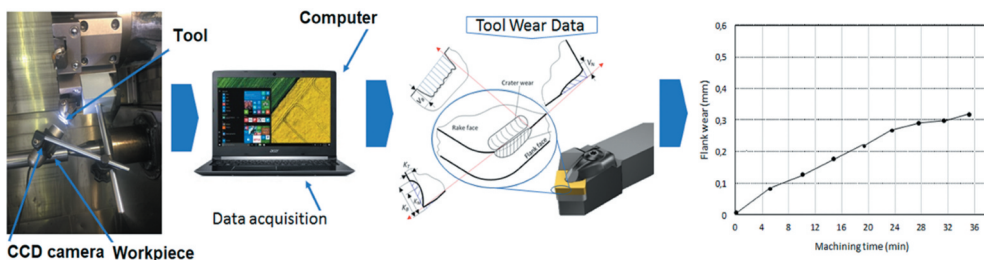
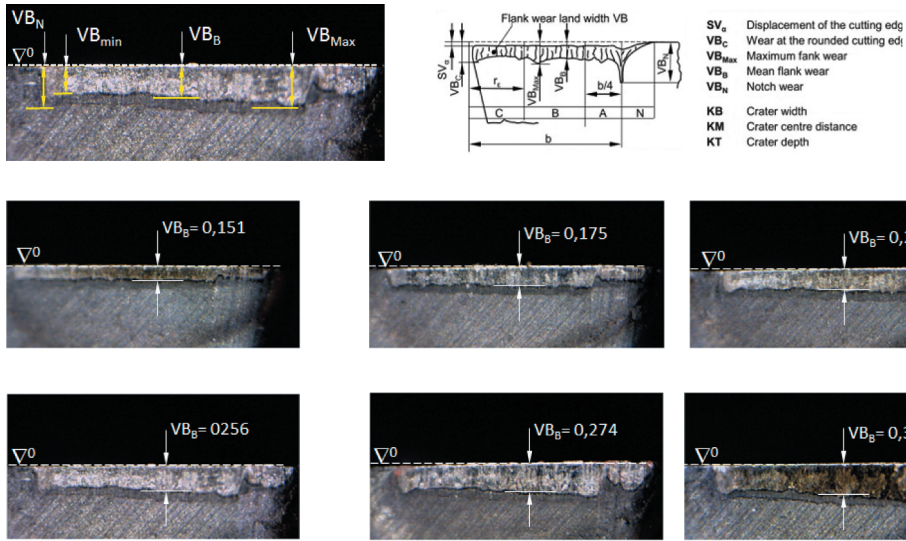


Figure 7. Experiments workflow.

Table 5. Example of flank wear VB_B progression measurement.



used as a cutting fluid [17]. The best performance was obtained with $V_c = 160$ m/min. A flank wear mark $VB_B = 0.3$ mm was set as the tool end life parameter. The experiments were performed using a CNC lathe maximum spindle speed of 4,000 rpm and 18.5 kW of power.

Before each experiment, the CCD camera was calibrated using an external precision scale, to ensure the accuracy of the dimensions obtained. Table 5 presents an example of Flank Wear VB_B progression measurement. Table 6 shows the number of trials and machining conditions of the tests performed.

4. Analysis of results

Figure 8 presents an example of the machining experiments results, where the flank wear (VB_B) progression was set against the cutting time. Based on the experiment results, an average behaviour was obtained for each cutting tool, in which the ratio is the lifetime of the cutting edge as a function of the flank wear.

Table 6. Number of trials performed by tested cutting tools.

Cemented carbides	Identification	V_c [m/min]	A_p [mm]	Feed [mm/rev.]	No of trials
NbC-Ni	900	160	1.5	0.1	3
	938	160	1.5	0.1	3
	959	160	1.5	0.1	3
	965	160	1.5	0.1	3
	967	160	1.5	0.1	5
	WC-Co	WC	160	1.5	0.1

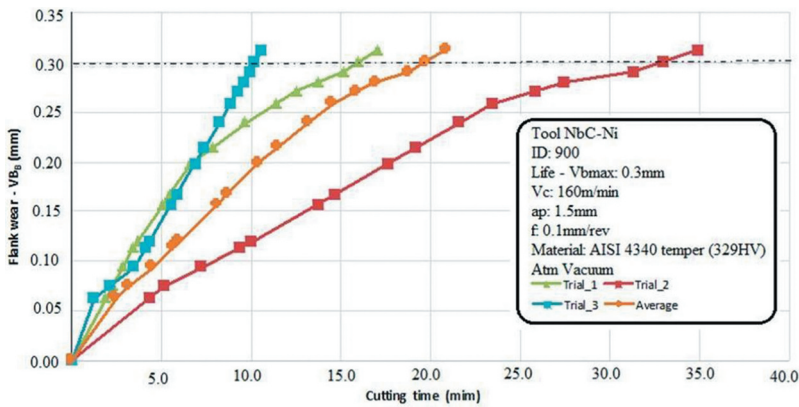


Figure 8. Flank wear VB_b versus cutting time – NbC-Ni_900.

The average behaviour for each cutting tool had a 95% confidence interval, and an error bar was also included to represent the uncertainty in the data based on the replicate tests. To confirm the statistical difference for the comparisons, an ANOVA analysis of variance was used. This allowed the researchers to test the means of the tests performed (repetitions) through their variance in order to confirm the differences between the NbC-Ni tools and the comparisons between the NbC-Ni and WC tools. The homogeneity test of variances was performed using the Bartlett test, shown in Table 7. In this test, the result showed that the variances are the same between the classes of the inserts, so the test used for the analysis of the means was Tukey’s. Table 8 summarises the ANOVA analysis of variance results.

As the p -value > 0.05 the null hypothesis is not rejected, so the variance is the same.

When the value of the statistic T value is very low, this means that the null hypothesis cannot be rejected and the averages should be considered as equals. When the statistic T value is very large, this means that the null hypothesis can be rejected, and the averages are totally different. The opposite is true for p -value, when $p < 0.05$, the null hypothesis can be rejected and the averages are different and when $p > 0.05$, the null hypothesis cannot be rejected and the averages can be equal. With regard to the values that are not highlighted in Table 7 the means can be totally different.

Table 7. Bartlett test.

Method	Test statistic	p-Value
Bartlett	6.56	0.255

Table 8. ANOVA results – flank wear $VB_b = 0.3$ mm – simultaneous Tukey tests.

Factor	T-Value	Adjusted P-value	Factor	T-Value	Adjusted P-value
WC x NbC-Ni_967	3.51	0.012	NbC-Ni_967 x NbC-Ni_938	4.27	0.009
WC x NbC-Ni_965	3.43	0.022	NbC-Ni_900 x NbC-Ni_965	-0.72	0.976
WC x NbC-Ni_959	0.17	1.000	NbC-Ni_900 x NbC-Ni_938	0.15	1.000
WC x NbC-Ni_938	-0.62	0.988	NbC-Ni_900 x NbC-Ni_959	3.32	0.040
WC x NbC-Ni_900	-0.75	0.971	NbC-Ni_965 x NbC-Ni_959	-1.76	0.523
NbC-Ni_967 x NbC-Ni_900	4.44	0.007	NbC-Ni_965 x NbC-Ni_938	3.30	0.044
NbC-Ni_967 x NbC-Ni_965	5.25	0.002	NbC-Ni_959 x NbC-Ni_938	0.88	0.944
NbC-Ni_967 x NbC-Ni_959	3.41	0.020			

In this analysis, it can be observed that the NbC-Ni_967 tool had an average performance which was totally different from all the other tools. The other tools had similar types of behaviour, due to high dispersion.

After obtaining the average lifetime of each cutting tool, it was possible to compare the developed NbC-Ni tools, as seen in Figure 9(a, b).

The development of the tools was carried out step by step, and each developed tool was tested and its results analysed to propose changes in the development of the next tool. The changes carried out were in the sintering process (temperature, heating temperature and sintering dwell time) and the weight percentage of the binder and niobium carbide.

The last tool developed in this step was NbC-Ni_967 where the binder content was reduced to 10% (Ni) and the NbC increased to 64%. The sintering process also had its sintering dwell time adjusted. The results from the mechanical properties were hardness 1460 HV and the KIC of 8.9 MPa.m^{1/2}. In relation to the machining performance, the cutting tool NbC-Ni_958 that had the best performance, the cutting tool NbC-Ni_967

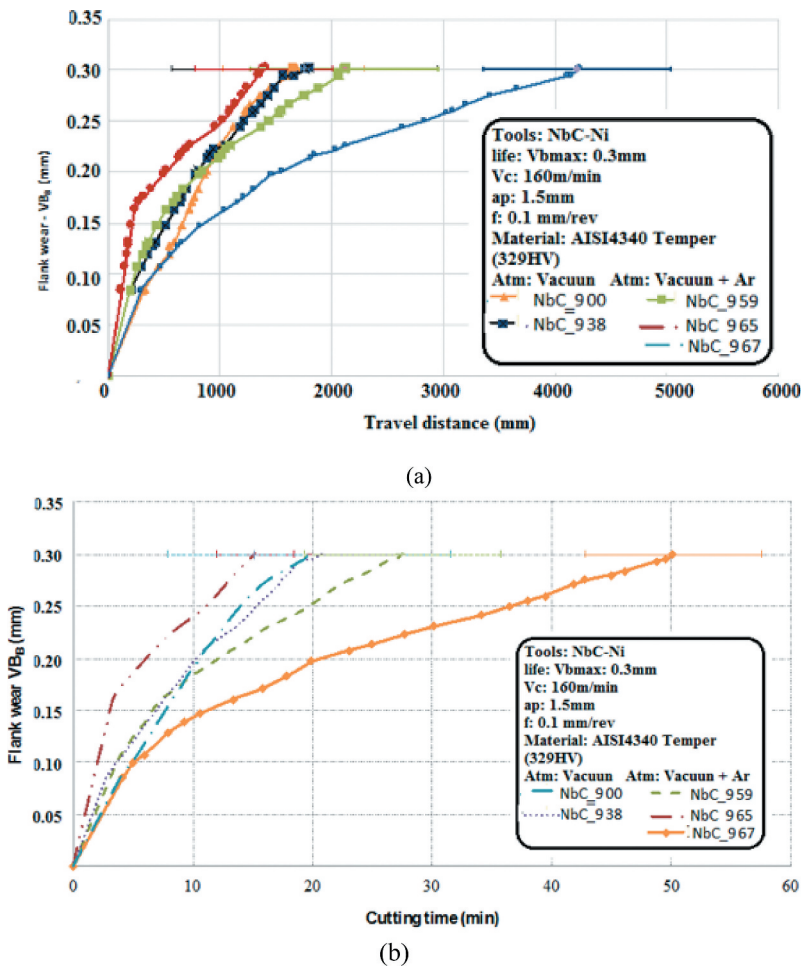


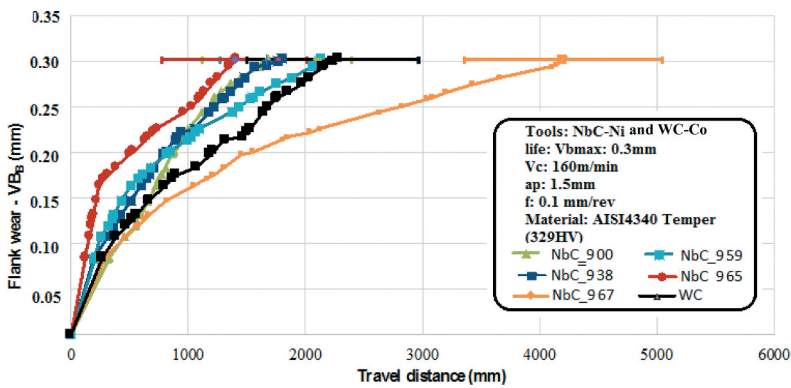
Figure 9. (a) Flank wear versus Travel distance; (b) Flank wear versus cutting time – machining tests with NbC-Ni cutting tools.

exceeded this by 88.1% (Figure 9(b)) in the cutting time, and almost double (98%) in relation to the travel distance (Figure 9(a)).

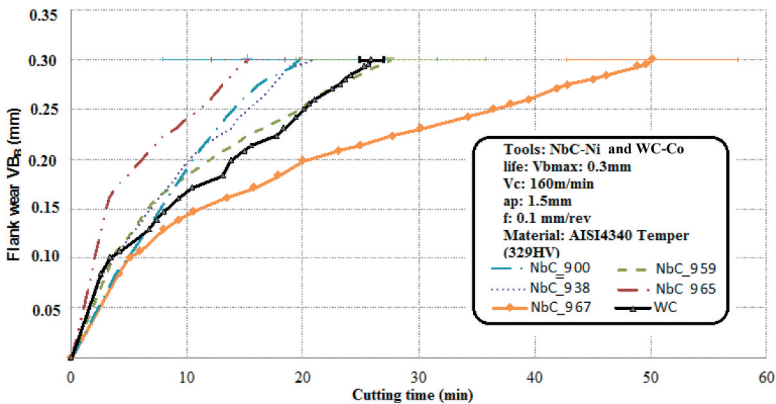
The second step of the analysis, Figure 10(a, b), was to compare the performance of the NbC-Ni-based cutting tools with the WC cutting tool, using the average performance obtained.

The NbC-Ni_900, 938 and 965 tools had a lower average performance than the WC tool. The NbC-Ni_959 had an average performance similar to the WC tool. The NbC-Ni_967 cutting tool was developed after data analysis of all the previous tests. This allowed the sintering process to be adjusted and also the chemical composition to be altered, reducing the binder and increasing the niobium carbide. These changes greatly improved the performance of this tool in relation to the WC cutting tool in the cutting time, making it 92.3% higher (Figure 10(b)) and in relation to travel distance, with a higher performance by 88.1% (Figure 10(a)).

Figure 11 presents the lifetime (min) performance in relation to the cutting edge wear that determined the end of life ($V_{B0} = 0.3$ mm) and the dispersion of the tool lifetime for each cutting tool tested. The vacuum-sintered inserts presented a similar average



(a)



(b)

Figure 10. Comparison of the average flank wear (V_{B0}) performance of NbC-Ni cutting tools versus WC-Co cutting tool – (a) Travel distance versus Flank wear; (b) Cutting time versus Flank wear.

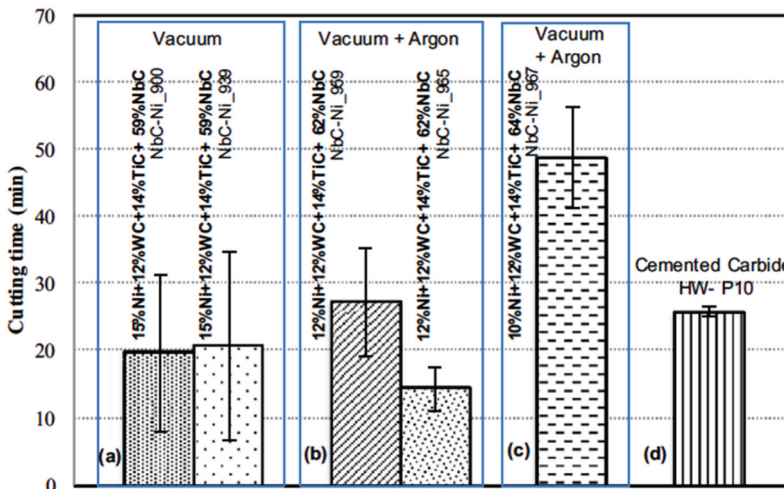


Figure 11. Tool life time for a flank wear $VB_B = 0.3$ mm versus the studied cutting tools.

performance, considering the cutting edge's lifetime during the machining process, according to ANOVA (Table 8). However, the dispersion of results was greater, as indicated in the error bar (Figure 11(a)). This high level of dispersion may be linked to a loss of nickel during vacuum sintering, which may promote microstructural heterogeneity. Compared with the reference insert (Figure 11(d)), the NbC-based inserts had a 21.8% lower average performance.

The sintered inserts under dynamic inert gas (Figure 11(b)), starting at 1380°C and with 12% Ni (nominal), showed distinct performances in the flank wear tests in the machining. The best performance was 89.5% over the average life of the cutting edge in relation to the NbC-Ni_965 insert, and this superior performance may be related to the longer time at the sinter level. The best performance, NbC-Ni_959, was 89.5% higher over the average life of the cutting edge in relation to the NbC-Ni_965 insert, and this better performance may be related to the longer threshold time. The machining performance reflects the values of mechanical properties: the sample produced with a longer threshold time, NbC-Ni_959, has a higher hardness and fracture toughness than that produced with the lower threshold time (NbC Ni_965). The longer the high temperature, the higher the dissolution of niobium, tungsten and titanium in the binder (nickel), increasing the hardness of the binder, which can increase the hardness of the insert. The NbC-Ni_959 insert showed an average performance which was similar to the reference cemented carbide insert according to statistical analysis using ANOVA (Table 8), but with a dispersion well above this. The cutting tool which was also produced in the sintering process under dynamic inert gas (Figure 11(c)), but with 10% Ni (NbC-Ni_967), showed a performance which was 88.8% better over the average cutting edge lifetime in the machining process in relation to the cutting tool WC-Co reference. However, the dispersion was again higher than that found for WC-Co and similar to those of the two samples produced in the same sintering process with 12% Ni.

Figure 12(a, b) shows an analysis which takes into consideration the average tool lifetime and hardness, average tool lifetime and fracture toughness. These analyses were performed for a $VB_B = 0.3$ mm.

It is possible to observe in Figure 12(a) that the NbC-Ni tool Vickers hardness below 1400 HV, highlighted, did not perform well. In relation to the fracture toughness, Figure 12 (b), there was a prominent region, where the results were promising, K_{IC} values between 8 and 9 $MPa \cdot m^{1/2}$, in relation to the performance in the average lifetime of the NbC-Ni tools.

The adhesion and abrasion analysis of the cutting edges were performed using SEM and EDS.

These analyses were also performed using optical microscopy. Through these analyses, it was possible to conclude that the mechanisms of wear on the tool based on NbC-Ni were abrasion and adhesion. Figure 13(a, b) and Table 9 show an example of the wear mechanisms that occurred in the tools of NbC-Ni (NbC-Ni_967).

5. Conclusions

The results obtained from the NbC-Ni cutting tools show the correct direction in their development. The sintering atmosphere was an important factor in the control of the homogeneity of NbC-Ni cutting tools. Samples of NbC-Ni cutting tools produced using only a vacuum atmosphere showed a greater dispersion in the tool life than the same samples produced in the sintering process with an argon dynamic atmosphere. The use of argon reduced the loss of nickel during the sintering process. However, it is possible to verify through micrographs that the NbC-Ni classes are heterogeneous for the two sintering processes.

The reduction of the nickel percentage (%wt) to 10% in weight (tool NbC-Ni_967), and the use of an argon dynamic atmosphere during sintering, increased the tool life the most when compared with all the other tools. Despite the tool life being higher than the WC-Co reference tool, this tool provides a lower dispersion of results than NbC-Ni_967 samples.

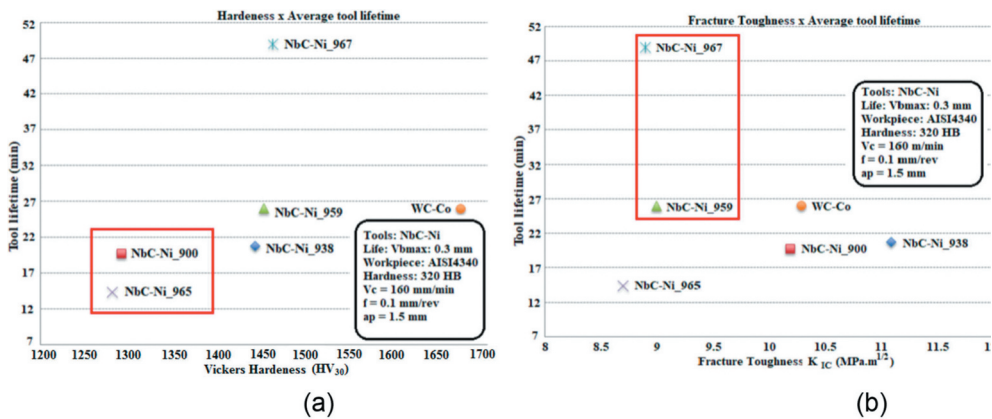


Figure 12. Performance comparison tools: (a) Hardness (HV) x Average tool life time (min); (b) Fracture toughness K_{IC} ($MPa \cdot m^{1/2}$) x Average tool life time (min).

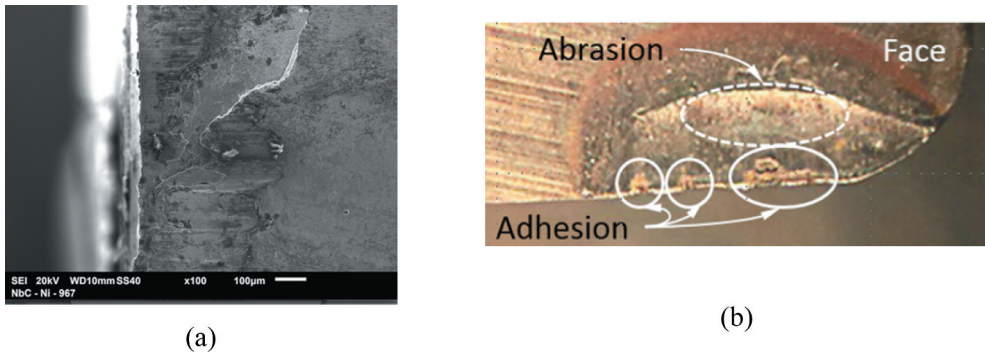


Figure 13. Wear Mechanisms (a) SEM; (b) Optical microscopy.

Table 9. Adhesion wear mechanism analysis – EDS (NbC-Ni_967).

Zone	Quantification result – mass percentage (%)							
	Fe	Si	Ti	Cr	Mn	Ni	Nb	W
01	13.9		12.7		3.5	3.0	57.7	9.2
02	10.0	4.3	10.9	0.4	6.3	1.3	58.1	8.7
03	4.4	8.0	10.3	0.5	6.9	2.0	58.8	9.1
04	1.8		13.6			9.9	62.6	12.1
05			13.5			9.9	64.4	12.2

One of the initial goals during the development of the NbC-Ni classes was to have the same fracture toughness and hardness as the WC-Co reference class. However, analysing the data found, [Figure 12\(a, b\)](#), it can be seen that the classes NbC-Ni and WC-Co are distinct in relation to the hardness and fracture toughness. However, the experiments show that a better performance can be achieved using NbC-Ni tools even when they have different properties than WC-Co.

The wear mechanisms observed during the machining process were mainly abrasion and adhesion. However, it is necessary to study further the mechanisms of wear during the machining process and to better understand the types of existing porosities and obtain better densification during the sintering process, in addition to studying the behaviour of plastic deformation. All of these analyses will help researchers to understand why NbC-Ni tools have a greater dispersion than WC-Co tools during their average useful life, in order to continue to improve the performance of these tools.

Acknowledgments

The authors would like to thank the CCM-ITA for all the equipment used to carry out the machining tests, EHT Consulting for supporting the manufacture of cutting tools used in this work, BRATS Co. for its support for the production of NbC-Ni cutting tools and LFS-USP for support in the hardness and metallographic tests.

Disclosure statement

No potential conflict of interest was reported by the authors.

References

- [1] Dehghanghadikolaei A, Fotovvati B, Mohammadian B, et al. Abrasive flow finishing of stainless 304 biomedical devices. *Res Dev Mater Sci.* **2018**;8:1–8.
- [2] Dehghanghadikolaei A, Mohammadian B, Namdari N, et al. Abrasive machining technique for biomedical device applications. *J Mater Sci.* **2018**;5:1.
- [3] Deng F, Tang Q, Li X, et al. Study on mapping rules and compensation methods of cutting-force-induced errors and process machining precision in gear hobbing. *Int J Adv Manuf Technol.* **2018**;97(9–12):3859–3871.
- [4] Klocke F. *Manufacturing process 1: cutting.* Berlin: Springer; **2011**.
- [5] Trent E, Wright P. *Metal cutting.* 4th ed. Oxford: Butterworth-Heinemann; **2000**.
- [6] Thummler F, Oberacker R. *Introduction to powder metallurgy.* UK: The institute of materials 1 Carlton House Terrace London; **1993**.
- [7] Smith GT. *Cutting tool technology: industrial handbook.* London: Springer; **2008**.
- [8] Kurlov AS, Gusev AI. Tungsten carbide: structure, properties and application in hardmetals. *Springer Series in Materials Science v.184*,**2013**.
- [9] Li A, Zhao J, Wang D, et al. Three-point bending fatigue behavior of WC-Co cemented carbides. *Mater Des.* **2013**;45:271–278.
- [10] Woydt M, Hohrbacher H, Vleugels J, et al. Niobium carbide for wear protection-tailoring its properties by processing and stoichiometry. *Metal Powder Report.* **2016**;1(4):265–272.
- [11] Woydt M, Hohrbacher H. The tribological and mechanical properties of niobium carbides (NbC) bonded with cobalt or Fe₃Al. *Wear.* **2014**;321:1–7.
- [12] Mohrbacehr H, Zhai Q. Niobium alloying in grey cast iron for vehicle brake discs. In: *Proc. Of Materials Science & Technology Conference.* **2011** Oct 16-20, Columbus, OH, ASM Int., p.434–445.
- [13] Uhlmann U, Hinzmann D, Kropidlowksi K, et al. Increased tool performance with niobium carbide based cutting materials in dry cylindrical turning. *8th CIRP Conference oh High Performance Cutting, Budapest* **2018**.
- [14] Franco E, Costa CE, Tsipas SA, et al. Cermets based on FeAl-NbC from composites powders: design of composition and processing. *Int J Refractory Metals Hard Mater.* **2015**;48:324–332.
- [15] Masalski TB. *ASM, binary alloy phase diagrams.* 2nd ed. Editors: T.B. Massalski, Okamoto, H., Subramanian, P. R., Kacprzak, L.. USA: ASM International; **1990**.
- [16] Vinitiskii IM. Relation between the properties of monocarbides of groups IV?V transition metals and their carbon content. *Soviet Powder Metallurgy Metal Ceramics.* **1972**;11(6):488–493.
- [17] Information on. [cited 2018 Sep 18]. http://www.cuttingfluids.com.mx/es/wpcontent/uploads/2014/09/Vasco_7000.pdf